

# MicroRNA-193 Pro-Proliferation Effects for Bone Mesenchymal Stem Cells After Low-Level Laser Irradiation Treatment Through Inhibitor of Growth Family, Member 5

Jue Wang,<sup>1-4</sup> Weicong Huang,<sup>1,4</sup> Yihe Wu,<sup>1-3</sup> Jianfeng Hou,<sup>1-3</sup> Yu Nie,<sup>1-3</sup> Haiyong Gu,<sup>1-3</sup>  
Jun Li,<sup>1,3</sup> Shengshou Hu,<sup>1-3</sup> and Hao Zhang<sup>1-3</sup>

The enhanced proliferation of mesenchymal stem cells (MSCs) can be helpful for the clinical translation of cell therapy. Low-level laser irradiation (LLLI) has been demonstrated as regulating MSC proliferation. MicroRNAs (miRNAs) are involved in various pathophysiologic processes in stem cells, but the role of miRNAs in the LLLI-based promotion of MSC proliferation remains unclear. We found that the proliferation level and cell cycle-associated genes in MSCs were increased after LLLI treatment in a time-dependent manner. Microarray assays revealed subsets of miRNAs to be differentially regulated, and these dynamic changes were confirmed by quantitative real-time polymerase chain reaction (qRT-PCR) after LLLI. miR-193 was the most highly up-regulated miRNA, and the change in it was related with the proliferation level. Gain-loss function experiments demonstrated that miR-193 could regulate the proliferation of MSCs, including human's and rat's, but could not affect the apoptosis and differentiation level. Blockade of miR-193 repressed the MSC proliferation induced by LLLI. By qRT-PCR, we found that miR-193, in particular, regulated cyclin-dependent kinase 2 (CDK2) expression. Bioinformatic analyses and luciferase reporter assays revealed that inhibitor of growth family, member 5 (ING5) could be the best target of miR-193 to functionally regulate proliferation and CDK2 activity, and the mRNA and protein level of ING5 was regulated by miR-193. Furthermore, the ING5 inhibited by small interfering RNA (siRNA) could up-regulate the proliferation of MSCs and the expression of CDK2. Taken together, these results strongly suggest that miR-193 plays a critical part in MSC proliferation in response to LLLI stimulation, which is potentially amenable to therapeutic manipulation for clinical application.

## Introduction

MESENCHYMAL STEM CELLS (MSCs), which are characterized by their ability to differentiate into multiple cell types, have been a popular cell resource for cell-based therapy [1]. Recent studies indicated that MSCs exhibit a reduced potential for proliferation in prolonged in-vitro culture [2]. Additionally, ageing can impair the biological properties of MSCs [3]. Therefore, to improve the efficacy of autologous cell therapy, applying a preconditioning approach that increases the proliferation ability of MSCs is essential. Furthermore, such a preconditioning approach can also significantly shorten the in vitro cell preparation time, thereby avoiding potential contamination during cell culture.

Low-level laser irradiation (LLLI) can exert strong effects on cell proliferation [4]. We previously found that LLLI could promote MSC proliferation, and demonstrated that lasers of 0.5 J/cm can promote proliferation and slightly affect MSC differentiation [5,6]. Until now, the mechanism of LLLI treatment for cell proliferation remains unclear. Several possible mechanisms and related signaling pathways have been found to be involved in LLLI treatment. It was found that LLLI can regulate mitochondrial signaling, activate calcium channels, and phosphorylate and release certain growth factors, thereby stimulating cell proliferation [4,7-9].

MicroRNA (miRNA) molecules can potentially regulate every aspect of cellular activity [10]. A subset of miRNAs has been found to have essential roles in the proliferation and differentiation of various types of stem cells [11]. miR-335

<sup>1</sup>State Key Laboratory of Cardiovascular Medicine, Fuwai Hospital and Cardiovascular Institute, Chinese Academy of Medical Sciences, Peking Union Medical College, Beijing, China.

<sup>2</sup>Department of Surgery, Fuwai Hospital and Cardiovascular Institute, Chinese Academy of Medical Sciences, Peking Union Medical College, Beijing, China.

<sup>3</sup>Research Center for Cardiac Regenerative Medicine, Ministry of Health, Beijing, China.

<sup>4</sup>Department of Thoracic and Cardiovascular Surgery, The First Affiliated Hospital of Wenzhou Medical College, Wenzhou, China.

has been demonstrated as regulating the proliferation, migration, and differentiation of MSCs [12]. miR-486-5p has been reported as regulating the proliferation of human adipose tissue-derived MSCs [13]. However, investigations into the role of miRNAs in LLLI pro-proliferation bio-modulation are lacking. Therefore, in the present study, we would like to evaluate the (i) expression profile of miRNAs after LLLI treatment in MSCs; (ii) related functions and pathways of the identified miRNA.

## Materials and Methods

The study was performed in conformity with the guidelines of humane use and care of laboratory animals published by NIH (No. 85-23, revised 1996), and the animal procedures were approved by the institutional ethics committee of Fuwai Hospital. Human MSCs (hMSCs) were isolated and cultured from 6 patients < 18 years old with simple congenital heart disease [3]. All the procedures were approved by the ethics committee at Fuwai Hospital, and all the enrolled patients signed the informed consent.

### Cell culture and preparation

Rat MSCs were isolated from male Sprague-Dawley rats (4 weeks; 60 g) obtained from the Institute of Laboratory Animal Science of the Chinese Academy of Medical Sciences (Beijing,

China) as previously reported [14]. MSCs were seeded at  $1.5 \times 10^3$  cells per well in 96-well culture plates for the proliferation assay, and at  $2.5 \times 10^5$  cells per dish in culture dishes (diameter, 35 mm) for miRNA microarray analyses and quantitative real-time polymerase chain reaction (qRT-PCR) analyses. Before laser irradiation, the culture medium was removed and replaced with fresh medium. The MSCs were then individually irradiated with a low-level laser. The control cells underwent the same procedure without laser irradiation. The cells were then incubated for different culture periods after irradiation, corresponding to the experimental purpose. The detailed study protocol is shown in Fig. 1A.

### Isolation and culture of hMSCs

The procedures were carried out as described in our previous study [3]. Briefly, 3–5 mL of bone marrow aspirate was taken from the sternum of patients during operations. Fresh bone marrow was stored in phosphate-buffered saline and heparin. After centrifugation, the residual cells were loaded onto Percoll solution. Then, the mononuclear cells were collected from the upper layer and interface, and the cells were cultured in Dulbecco's modified Eagle's medium (DMEM; Gibco, Grand Island, NY) supplemented with 10% fetal bovine serum (FBS; Gibco BRL, Carlsbad, CA). The proliferation of hMSCs was measured by 5-bromo-2'-deoxyuridine (BrdU) incorporation assay and 3-(4,5-dimethylthiazol-2-yl)-

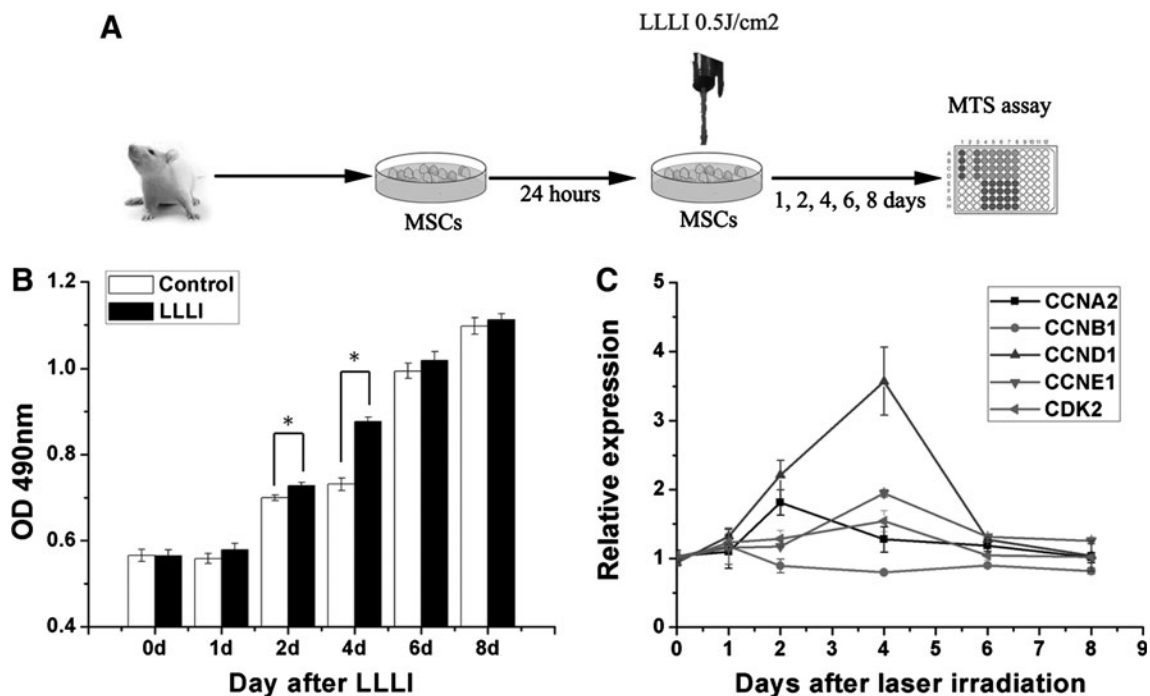


**FIG. 1.** Low-level laser irradiation (LLLI) promotes mesenchymal stem cell (MSC) proliferation and increases cell cycle-associated gene expression. **(A)** MSCs isolated from rats were passaged and placed in wells for 24 h. The MSCs were individually irradiated with a low-level laser. Proliferation of the MSCs was measured by 3-(4,5-dimethylthiazol-2-yl)-5-(3-carboxymethoxyphenyl)-2-(4-sulfophenyl)-2H-tetrazolium (MTS) analyses. **(B)** MSCs were irradiated by LLLI at an energy density of 0.5 J/cm<sup>2</sup> (test group) and 0 (control group). After LLLI, the MTS assay was carried out, and OD490 was compared at day 0, 1, 2, 4, 6, and 8. Mean  $\pm$  standard error of the mean (SEM). \* $P < 0.05$  compared with control groups ( $n = 3$ ). **(C)** The expression of cyclin A2 (CCNA2), cyclin B1 (CCNB1), cyclin D1 (CCND1), cyclin E1 (CCNE1), and cyclin-dependent kinase 2 (CDK2) was detected by quantitative real-time-polymerase chain reaction (qRT-PCR) in the MSCs treated by LLLI in the same process as **(B)**. CCNA2 was up-regulated on day 2, and CCND1/CCNE1 and CDK2 were up-regulated on day 4, compared with the control groups ( $n = 3$ ).

5-(3-carboxymethoxyphenyl)-2-(4-sulfophenyl)-2H-tetrazolium (MTS) assay 48 h after transfection.

### Laser irradiation

Laser irradiation was carried out as described in our previous report [5]. Briefly, laser irradiation was undertaken with a diode laser (KDL-300; Beijing KeDian Microwave Electronics Co., Beijing, China) operating at a wavelength of 635 nm (red light). The output power was kept constant at 60 mW. We previously found 0.5 J/cm<sup>2</sup> to be the appropriate laser irradiation dose that induces MSC proliferation [5]. Therefore, an energy density of 0.5 J/cm<sup>2</sup> was applied using a power density of 6.61 mW/cm<sup>2</sup>, a lens-plate distance of 89 mm, and an irradiation time of 75 s. To fit to culture dishes of diameter 35 mm, the width of the laser beam was adjusted to 34 mm. Rat MSCs were seeded in wells away from each other to avoid overlapping or scattered irradiation. Black backgrounds in irradiated areas were used to minimize light reflection, and all procedures were done on a super-clean bench.

### Proliferation assay

MSC proliferation was determined by the colorimetric MTS assay (CellTiter 96<sup>®</sup> AQueous One Solution Cell Proliferation Assay; Promega, Madison, WI) and a colorimetric BrdU Cell Proliferation enzyme-linked immunosorbent assay (ELISA) kit (Calbiochem, Gibbstown, NJ). In irradiation experiments, experiment and control rat MSCs were seeded in culture plates and assayed 0, 1, 2, 4, 6, and 8 days after LLLI. The culture medium was replaced every 2 days. The MTS assay was undertaken by following a protocol [5]. The absorbance of the obtained dye was measured at 490 nm using a microplate reader (Model 680; BioRad, Tokyo, Japan). In addition, a Colorimetric BrdU Cell Proliferation ELISA kit (Calbiochem) was used as previously described [15]. Briefly, experiments were undertaken as just described: 24 h after transfection, the cells were labeled with BrdU for another 12 h, and DNA syntheses were measured using a BrdU ELISA kit according to the manufacturer's instructions.

### miRNA microarray analyses

The significant difference of proliferation level between LLLI treatment and the control group was observed at day 4, so we chose this time point to analyze miRNA expression by miRNA microarray. RNA was extracted using the TRIZOL method (Invitrogen, Carlsbad, CA), and miRNAs were isolated with a mirVana miRNA Isolation kit (Ambion/Applied Biosystems, Foster City, CA). miRNA profiling of LLLI *versus* control MSCs was done using a miRNA microarray, and 2 biological replicates were employed for each condition. miRNA microarray analyses were undertaken by CapitalBio Company with the Rat microRNA Array 2.0 system (Affymetrix Japan Co., Tokyo, Japan) according to the Affymetrix GeneChip Expression Analysis Technical Manual and all 389 rat miRNA probes. Details of the preparation and analysis of samples are described elsewhere [16]. Gene ontology analyses were done for genes regulated by >1.2-fold ( $P < 0.05$ ), showing a correct hybridization signal on the 4 arrays. Hierarchical clustering was carried out by a Cluster 3.0 system using differentially expressed genes. Cluster data were processed and visualized using Java Treeview software.

### Quantitative real-time polymerase chain reaction

RNA was extracted as just described. qRT-PCR was done using the ABI 7300HT system (Ambion/Applied Biosystems). miRNA RT-PCR was undertaken using a TaqMan MicroRNA Reverse Transcription kit (Ambion/Applied Biosystems) and TaqMan probes for hsa-miR-15b, hsa-miR-133b, hsa-miR-193, hsa-miR-224, hsa-miR-320, and hsa-miR-23a (Ambion/Applied Biosystems), based on the protocols from the TaqMan MicroRNA assay (Ambion/Applied Biosystems). Expression levels were normalized to U6 snRNA (Ambion/Applied Biosystems). miRNA levels were quantified with the  $2^{-\Delta\Delta C_t}$  relative quantification method. All TaqMan miR assays were carried out in triplicate.

SYBR green chemistry was employed for analyses of the expression levels of cyclin-dependent kinase 2 (CDK2), cyclin A2 (CCNA2), CCNB1, cyclin D1 (CCND1), cyclin E1 (CCNE1), and inhibitor of growth family, member 5 (ING5), CCAAT-enhancer-binding protein (C/EBP), peroxisome proliferator-activated receptors gamma (Pparg), runt-related transcription factor 2 (Runx2), octamer-binding transcription factor 4 (Oct4), sex determining region Y-box 2 (Sox2) mRNA. Glyceraldehyde-3 phosphate dehydrogenase (GAPDH) was used as the housekeeping control. All primers for the SYBR green reactions are shown in Supplementary Table S1 (Supplementary Data are available online at [www.liebertonline.com/scd](http://www.liebertonline.com/scd)). Double-stranded complementary DNA was synthesized from 1 µg total RNA samples using a Promega RT Reagent Kit (Promega Biotechnology, Beijing, China) according to the manufacturer's instructions. PCR reactions were carried out in a 20 µL reaction volume using a Power SYBR Green PCR Master Mix (Ambion/Applied Biosystems).

### Western blot analyses

Samples from cultured MSCs were homogenized and lysed. ING5 (1:1,000 dilution; Proteintech, Chicago, IL), Proliferative cell nuclear antigen (PCNA; 1:1,000 dilution; Santa Cruz, CA), and GAPDH (1:6,000 dilution; Sigma-Aldrich, St Louis, MO) were used to determine protein expression. Experiments were undertaken using standard procedures as previously described [15]. All western blots were quantified by densitometry using the Quantity One program (BioRad, Hercules, CA).

### Delivery of miRNA inhibitors/mimics

Transfection using the SiPORT NeoFX Transfection Agent (Ambion/Applied Biosystems) was undertaken according to the manufacturer's protocols. Briefly, MSCs were transfected with miRNA mimic and inhibitor or small interfering RNA (siRNA) for ING5 (GenePharma Co. Ltd., Shanghai, China) in the suspension situation before detaching and to the final concentration of 50 nM. All the sequences of miRNAs are shown in Supplementary Table S2. Samples were collected 48 h after miRNA transfection. To detect the differentiation of MSCs, the samples were collected 6 days after the transfection.

### Immunocytochemistry

Immunocytochemistry was done according to a standard protocol. Briefly, cultured MSCs were fixed in 4% paraformaldehyde and permeabilized with ice-cold methanol. Cells



were blocked with 5% serum from the same species as the secondary antibody. MSCs were then incubated with primary antibody Ki-67 (1:100; Abcam, Cambridge, UK) overnight and stained with fluorochrome-conjugated secondary antibodies for 30 min. MSCs were mounted in VectaShield (Vector Laboratories, Peterborough, UK) with 4',6-diamidino-2-phenylindole (DAPI) to visualize nuclei. The terminal deoxynucleotidyl transferase dUTP nick end labeling (TUNEL) assay was carried out using an In Situ Cell Death Detection kit (Roche, Basel, Switzerland) according to the manufacturer's protocols. DAPI was used for nuclear counterstaining. Images were captured using an inverted microscope (BX61; Olympus, Tokyo, Japan). The percentage of Ki-67- or the number of DAPI-positive cells was counted in 9 regions and divided by the DAPI number.

**Luciferase reporter assays**

The luciferase reporter assay was carried out as previously described [17]. Briefly, the fragment of the 3' untranslated region (3'-UTR) of ING5 mRNA containing the putative (WT) or mutated (MU) miR-193 binding sequence was used to construct the vectors. The sequences of the miR-193 binding site and mutant site were: WT (5'-ATTTAATAATT CAGTGGCCAGT-3', from 97 to 118bp of the 3' UTR region) or MU (5'-ATTTAATAATTCAGTCCGGUCA-3'). The miR-193 binding sites were constructed using the *SacI* and *HindIII*

restriction sites of pMIR-REPORT. Overall, 293T cells were transfected with Lipofectamine 2000 (Invitrogen) according to the manufacturer's instructions. The cells were further grown in DMEM containing 10% FBS. Relative luciferase measurements were made 48 h after the transfection using the dual Luciferase Reporter Assay System (Promega) using a luminescence counter.

**miRNA target search**

Target genes for miRNAs were predicted using open-source software TargetScan 5.2 ([www.targetscan.org](http://www.targetscan.org)).

**Fluorescence-activated cell sorting analyses**

Cells undergoing apoptosis were detected by fluorescence-activated cell sorting (FACS) analyses. Briefly, the cells were cultured in low-serum DMEM for 48 h after the transfection. They were then dyed with an Annexin VAPC Apoptosis Detection Kit (eBioscience, San Diego, CA) for 30 min followed by an FACS analyses with FACS Calibur (BD Biosciences, Franklin Lakes, NJ) according to the manufacturer's protocols.

**Differentiation assays**

The rat MSCs were transfected with pre-miR-193 or anti-miR-193 and negative control; 2 days after the transfection, the medium was changed by conditioning the medium for 10

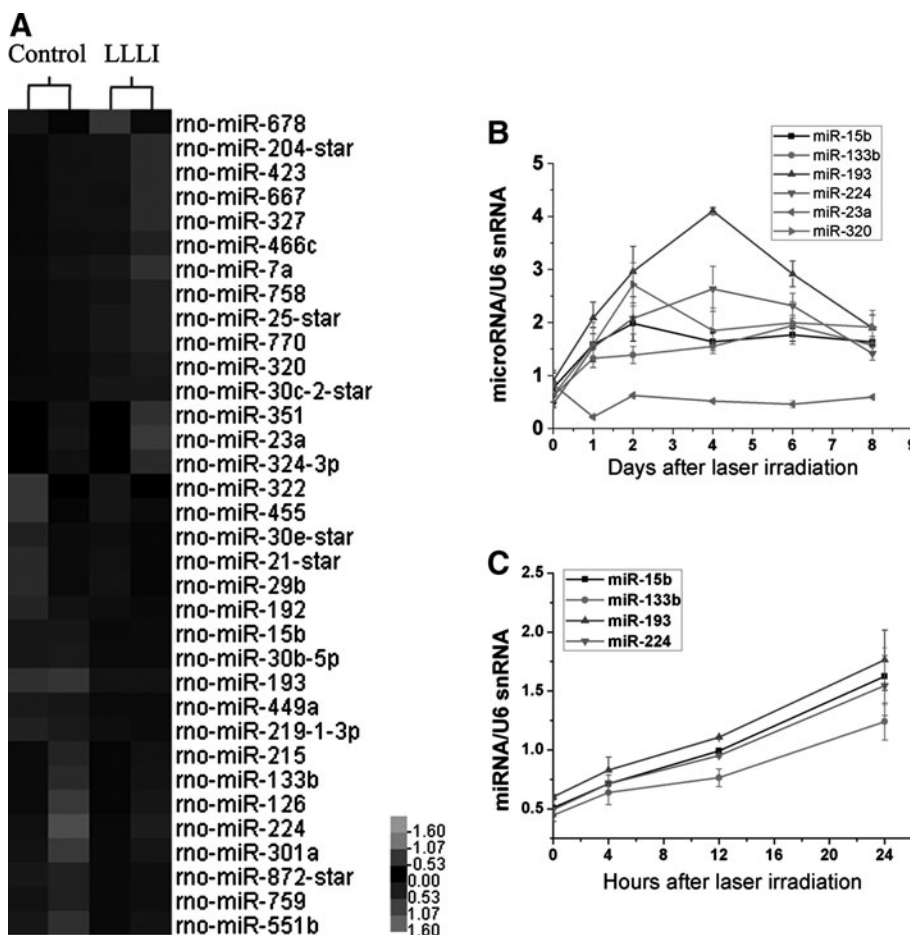


**FIG. 2.** Profiling of microRNA (miRNA) expression after LLLI treatment in MSCs. **(A)** Expression patterns of differentially regulated miRNAs in MSCs 4 days after the irradiated LLLI were identified by global microarray analyses. A heat map showing miRNAs regulated between LLLI treatment and control groups (LLLI and control) in MSCs with a cutoff point of 1.2 ( $P < 0.05$ ) (gray represents lower-than-median expression levels; black represents equal-to-median expression levels; and black represents higher expression levels). **(B)** Day-wise temporal regulation of miRNAs after LLLI treatment in MSCs was analyzed by qRT-PCR. The expression levels of each miRNA are normalized to U6 and represented as a fold change relative to the control group ( $n = 3$ ). **(C)** Hour-wise temporal regulation of miRNAs in MSCs after LLLI, in the same process as that in **(B)** ( $n = 3$ ).

TABLE 1. EXPRESSION OF MICRORNAs IN LOW-LEVEL LASER IRRADIATION-TREATED MESENCHYMAL STEM CELLS DETECTED BY MICROARRAYS

Up-regulation	Down-regulation
miR-30e-star	miR-204-star
miR-15b	miR-7a
miR-30b-5p	miR-423
miR-322	miR-678
miR-215	miR-25-star
miR-449a	miR-327
miR-126	miR-351
miR-133b	miR-23a
miR-21-star	miR-667
miR-455	miR-770
miR-759	miR-324-3p
miR-872-star	miR-30c-2-star
miR-29b	miR-758
miR-192	miR-320
miR-219-1-3p	miR-466c
miR-301a	
miR-551b	
miR-224	
miR-193	

days. The procedures were carried out as described earlier [13]. Adipogenic differentiation was induced by an adipogenic medium (5% FBS, 1 mM dexamethasone, 0.5 mM/mL 3-isobutyl-1-methylxanthine, and 200 mM indomethacin in alpha-modified Minimal Essential Medium [a-MEM]). Osteogenic differentiation was induced through the osteogenic medium (10% FBS, 0.1 mM dexamethasone, 10 mM  $\beta$ -glycerophosphate, and 50 mM ascorbic acid in a-MEM). After 10 days of differentiation, the cells were collected to extract RNA and to perform qRT-PCR.

### Statistical analyses

Data are the mean  $\pm$  standard error of the mean. Differences among the groups were tested by 1-way analysis of variance. Statistical analyses between 2 groups were evaluated based on the Student's *t*-test. Differences between the groups were evaluated using Fisher's least-significant difference test.  $P < 0.05$  was considered significant.

## Results

### LLLI promotes MSC proliferation and increases cell cycle-associated gene expression

Cultured MSCs were detected by flow cytometric analyses of expressed surface antigens as comprising a unique phenotypic population as shown in our previous study [18,19]. The number of viable cells increased rapidly after LLLI treatment from day 1 to day 4, and peaked at day 6 (Fig. 1B). A positive difference was observed at day 2 and day 4 after treatment compared with nonirradiated cells, which was consistent with previous reports [5].

Cell cycle-specific proteins can be elevated by LLLI treatment [9]. We found that CCND1, CCNE1, and CDK2 were up-regulated at day 4 after LLLI treatment, and CCNA2 was up-regulated at day 2, and the changes were time dependent (Fig. 1C).

### miRNA expression after LLLI treatment

To determine changes in miRNA expression, we identified global changes in miRNA expression patterns after LLLI treatment (Fig. 2A). A total of 34 miRNAs were differentially regulated after LLLI treatment: 19 miRNAs were up-regulated, and 15 miRNAs were down-regulated (Table 1). We chose the most significantly changed miRNAs and previously reported pro-proliferation miRNAs as target miRNAs, including miR-15b, -23a, -133b, -193, -224, and -320. These changes were detected by qRT-PCR analyses in a time-dependent mode. Surprisingly, most of the significantly up-regulated miRNAs were initially down-regulated after laser irradiation, and then, they gradually increased. The expression level of miRNAs peaked at day 2 and day 4, and most of them attenuated at day 6 and were back to normal levels at day 8 (Fig. 2B, C). We also found miR-193 was the most significantly up-regulated miRNA.

Using online prediction software (TargetScan), the 6 differentially expressed miRNAs (miR-15b, miR-23a, miR-133b, miR-193, miR-224, and miR-320) were analyzed for proliferation with potential 102 target genes (Table 2).

### Monitoring the proliferation of MSCs induced by miRNA

To determine the role of target miRNAs in MSC proliferation, antagomirs and mimics of miRNAs were transfected into MSCs.

TABLE 2. POSSIBLE TARGETS OF MICRORNAs

MicroRNA	Predicted target genes
miR-15b	AXIN2, SMAD2, B4GALT1, CHEK1, CCNE1, MAPRE1, MAPK3, SNF1LK, APLN, CXCL10, IHH, MAP2K1, PIM1, SH2D2A, TPT1, MFN2, PDCD4, ESRRA
miR-23a	RAP1A, DMTF1, MAF, PDCD4, DAB2IP, ALDH1A2, MARCKSL1, IL3, BTBD14B, IL11, IHH, MACF1, PKIA, CCND1, STAT5B, DLG1, RBBP9, PLAUG, MTF, NEK6, CCNG1, CCNH, MAPRE1, RAD17, NFIB, TGIF1, MADD, TXNRD1, SOX11, RAP1B
miR-133	PRRX1, ID4, PTH1R, NFIB, ARL3, CALM3, MAEA, LZTS2, GAS2, FGF1, FURIN, MAFG
miR-193	CNBP, KRAS, KIT, IGFBP5, LGR4, CALM3, SPECC1L, ING5
miR-320	PDCD4, RAP1A, RASSF2, TSC1, E2F1, ID4, S1PR1, EREG, HDAC4, PTEN, CDK6, CDKN1C, AURKB, CALM3, CLASP2, PLK3, PPP1CB, CCND2, CNBP, ID4, EIF5A2, MYH10
miR-224	STAT5B, IRS2, TRIB1, SMAD4, NFIB, STAT5B, ST8SIA1, TIAL1, SOX11, IRS2, MAFG, RALBP1

Using the online prediction software TargetScan, 102 possible proliferation-related target genes were predicted for the 6 broadly conserved microRNAs (miR-15b, miR-23a, miR-133, miR-193, miR-320, and miR-224).

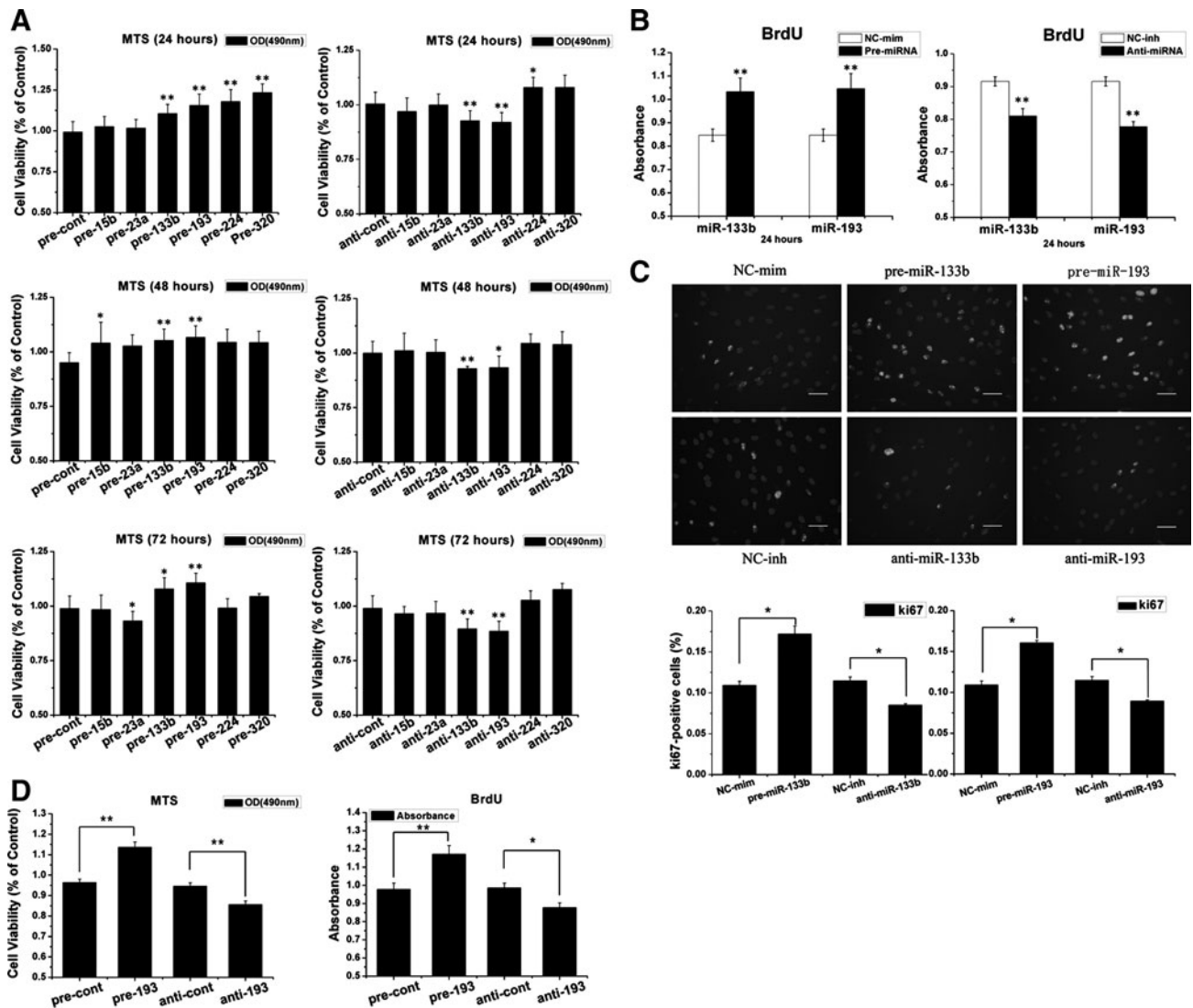
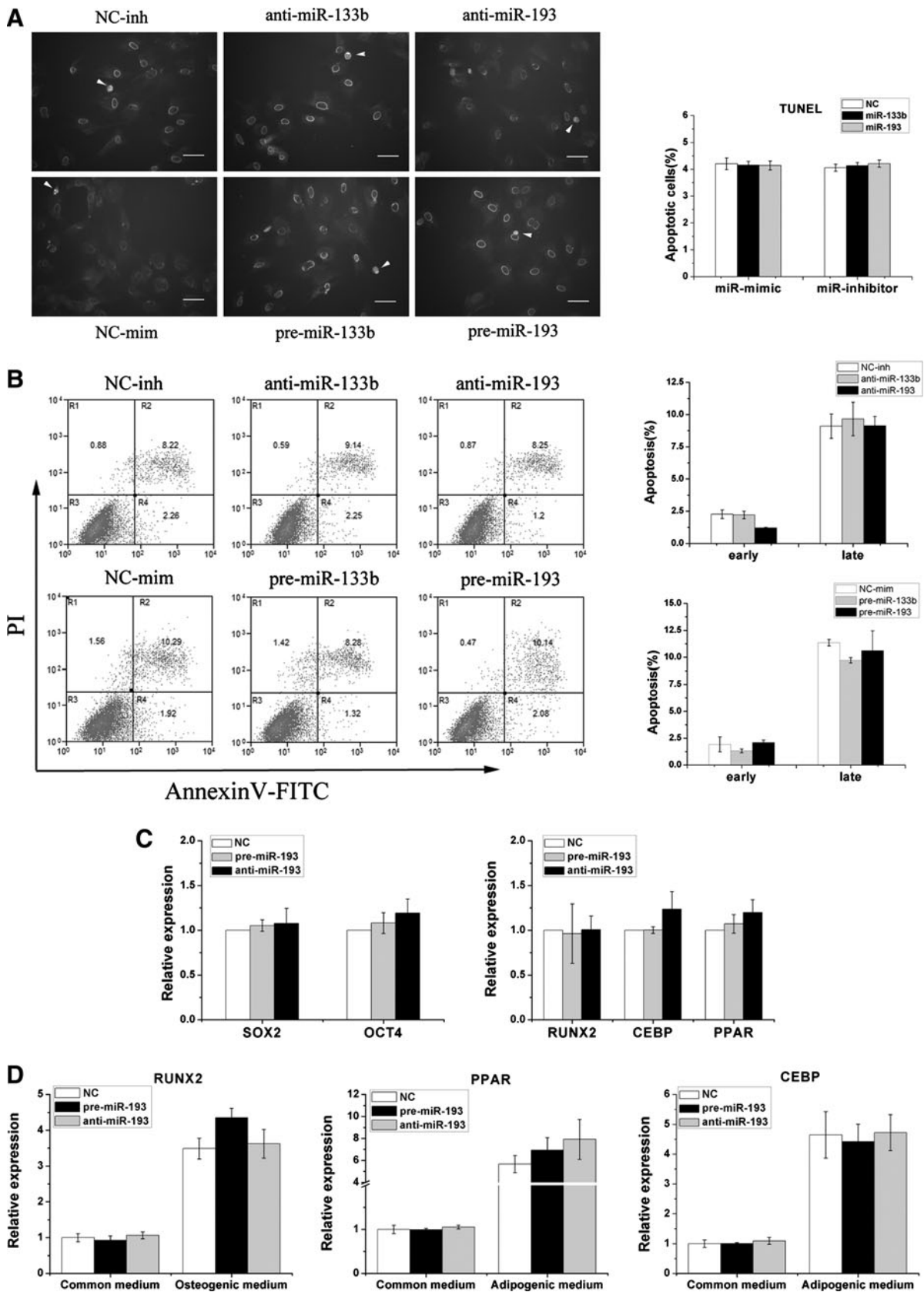


**FIG. 3.** miR-133b/193 regulates MSC proliferation. (A) Cells were transfected with different miRNAs, and their viability was assessed by the MTS assay at different times (24, 48, and 72 h) after transfection. Results are the percentage of control (taken as 100%). Overall, there were significant differences among miR-193 and miR-133b compared with the control at different times ( $n=3$ ). (B) 5-bromo-2'-deoxyuridine (BrdU) incorporation was used to detect the proliferation of MSCs transfected by miR-193 and miR-133b ( $n=3$ ). (C) Representative images of Ki-67 immunostaining in MSCs transfected with miR-193 and miR-133b as well as empty xenografts that analyze cell proliferation. Bar = 50  $\mu\text{m}$  white indicates ki-67-positive cells; gray indicates staining by 4',6-diamidino-2-phenylindole (DAPI). The percentage of Ki-67-positive cell number was divided by the DAPI number in the same zone. Mean  $\pm$  SEM. \* $P < 0.05$ , \*\* $P < 0.01$  compared with control groups. ( $n=3$ ). All experiments were repeated thrice (technical triplicates) with biological triplicates. (D) Proliferation level of human MSCs (hMSCs) that were transfected with miR-193 or its inhibitor was detected by BrdU incorporation and MTS assay ( $n=6$ ). Results show that miR-193 could promote hMSCs proliferation.

**FIG. 4.** miR-193 cannot regulate MSC apoptosis and differentiation. (A) Analyses of in-situ terminal deoxynucleotidyl transferase dUTP nick end labeling (TUNEL) detection of apoptotic cells in MSCs transfected with miR-193 and miR-133b mimics or inhibitors. Representative images of the TUNEL assay (left panel), and TUNEL-positive cells (right panel) of transfected miRNAs and control MSCs. White arrows indicate TUNEL-positive cells. Bars: 50  $\mu\text{m}$ . Mean  $\pm$  SEM,  $n=3$ . (B) Apoptosis in MSC cells was detected by flow cytometry. Cells were transfected with miR-193 and miR-133b mimics or inhibitors, and cell suspensions were stained with annexin V/propidium iodide (PI) and subjected to flow cytometric analyses. The apoptosis rate was quantified (right panel). There were no significant differences between transfected MSCs and those in the control groups. Mean  $\pm$  SEM,  $n=3$ . (C) The pluripotency of undifferentiated MSCs was detected by the expression of OCT4 and SOX2. The differentiation of MSCs was detected by RUNX2 (marker of osteogenic), CEBP, and PPAR (marker of adipose) by qRT-PCR. Mean  $\pm$  SEM,  $n=3$ . (D) After transfection, the MSCs were transferred to either osteoblast- or adipocyte-inducing media for 10 days. Cells were collected, and the differentiation of MSCs was analyzed by qRT-PCR as mentioned in (C).





The transfection rate was confirmed by the fluorescence in the MSCs from FAM<sup>TM</sup> dye-labeled miRNA, and by qRT-PCR assays. The expression levels of miRNA clearly increased (>10-fold) and decreased (<10%) after miRNA mimic and inhibitor transfection, respectively (Supplementary Fig. S1A, B). The overexpression of miR-133b, miR-193, miR-224, and miR-320 in MSCs could moderately increase cell viability 24 h after the transfection compared with cells transfected with a control mimic (Fig. 3A). However, in the inhibitor transfection group, only anti-miR-193 or anti-miR-133b could significantly inhibit cell proliferation. Furthermore, in the 48-h and 72-h groups after transfection, only miR-133b and miR-193 had standard functions that regulate MSC proliferation in the gain-and-loss-of-function experiment.

To confirm that miR-133b and miR-193 regulate MSC proliferation, we used the BrdU incorporation assay. miR-193 and miR-133b could significantly regulate the proliferation of MSCs (Fig. 3B). Furthermore, we detected Ki-67 protein expression in MSCs 24 h after the transfection by immunocytochemistry. The overexpression of miR-193 and miR-133b could significantly up-regulate Ki-67 expression in MSCs, and inhibiting them decreased Ki-67 expression (Fig. 3C).

To further check whether miR-193 could regulate the proliferation of hMSCs, we transfected the hMSCs with miR-193 and its inhibitor; then, we assessed the proliferation by MTS and BrdU incorporation. We found that pre-miR-193 could promote the proliferation of hMSCs, contrary, inhibit miR-193 would suppress the proliferation of hMSCs (Fig. 3D).

*miR-133b and miR-193 cannot regulate MSC apoptosis and differentiation*

In-situ TUNEL labeling showed that there was no significant difference in apoptosis levels between the miR-193/miR-133b transfect and control groups (Fig. 4A). To further confirm the role of miR-193 and miR-133b in MSC apoptosis, a flow cytometric assay indicated that there was no significant difference between early [annexin V-fluorescein isothiocyanate (FITC)-positive] and late apoptotic/necrotic (annexin V-FITC/propidium iodide-positive) cells (Fig. 4B). To clarify whether miR-193 could affect the MSCs differentiation, we examined the effects of miR-193 on the expression

of Sox2 and Oct4 transcription factors, which are known to be involved in the pluripotency and self-renewal of undifferentiated stem cells [20], and in the expression of genes that are specific to the adipose (CEBP and PPARg) or osteogenic lineage (RUNX2) [21]. As shown in Fig. 4C, the transfected miR-193 in MSCs maintained for 6 days did not show significant differences in the expression of these genes by qRT-PCR. Furthermore, MSCs that were cultured in either an osteoblast- or an adipose-inducing medium for 10 days after transfection with miR-193 or its inhibitor also did not show significant differences of these genes in each of these groups (Fig. 4D).

*Blockade of miRNA inhibits the MSC proliferation induced by LLLI*

Compared with nontreated cells, a significant increase in cell viability was observed in MSCs treated with LLLI. The viability of cells treated with LLLI in conjunction with anti-miR-133b and anti-miR-193 transfection was significantly decreased compared with that of cells with LLLI treatment (Fig. 5). These results suggested that miR-133b and miR-193 play crucial roles in cell proliferation induced by LLLI.

*miR-193 and miR-133b regulate the expression of cell-cycle genes and the miR-193 target 3' UTR of ING5*

The overexpression of miR-193 increases the expression of CDK2; inhibiting miR-193 would decrease CDK2 expression (Fig. 6A). In addition, the overexpression of miR-133b regulates the expression of CCND1 and CDK2 (Fig. 6B). These results indicated that miR-193 and miR-133b could regulate the proliferation of MSCs through several cell-cycle genes.

The conserved target genes of miR-193 were predicted and searched using an miRNA database to further elucidate the function of miR-193-based regulation of MSC proliferation. Among the candidates, ING5 was chosen as an appropriate target of miR-193. The expression of the ING5 protein and mRNA in miR-193-overexpressed MSCs was almost 50% lower than that in control cells 48 h after the transfection. In

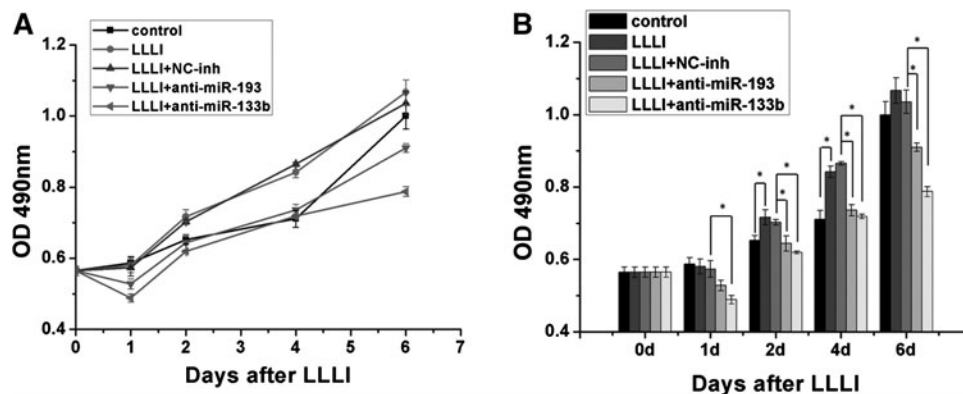
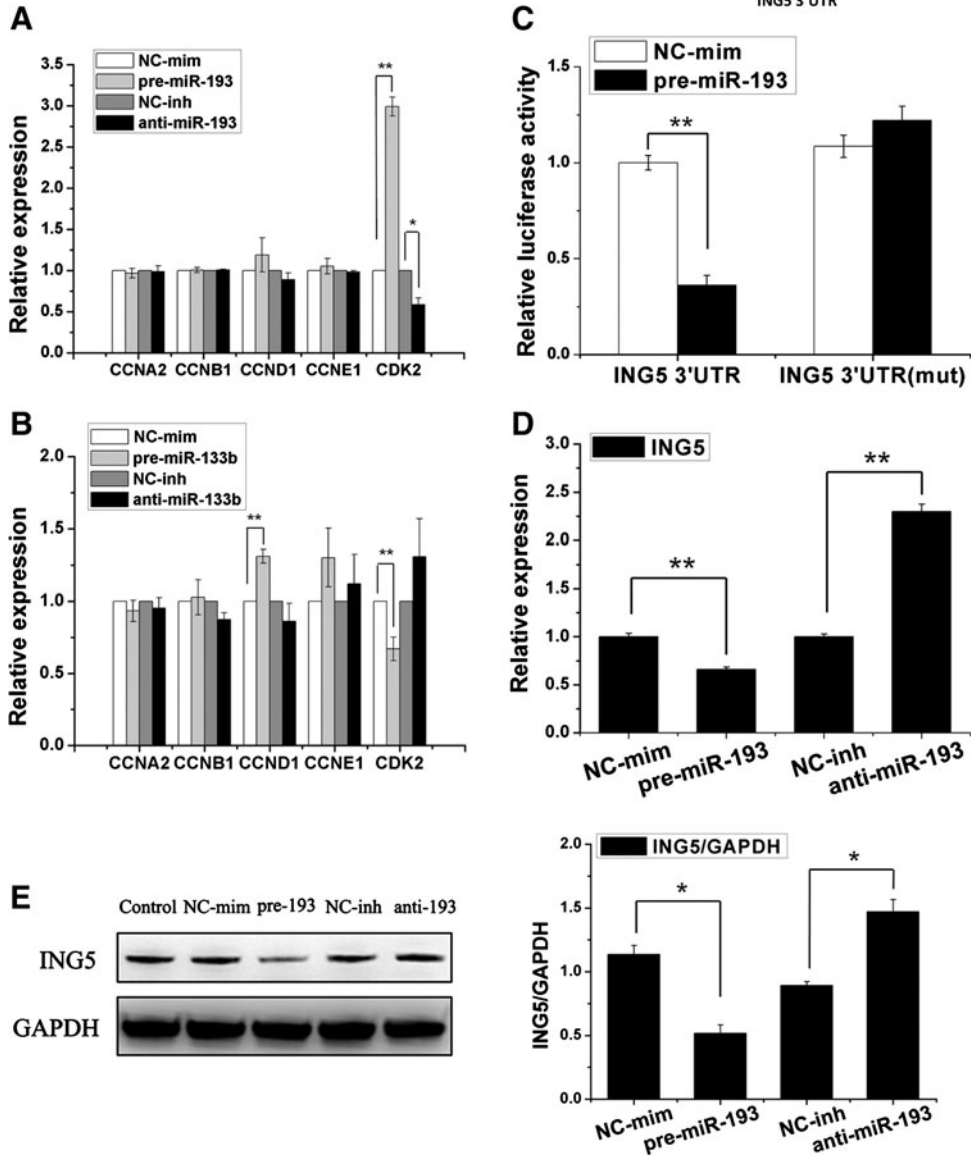


**FIG. 5.** Effects of miR-193, miR-133b inhibitors on LLLI-induced cell proliferation. (A) Cell viability was assessed by the MTS assay 1, 2, 4, and 6 days after 0.5J/cm<sup>2</sup> LLLI in the presence or absence of miR-193/133b inhibitors. Changes in cell viability over time are shown in the left panel. (B) Differences between each group are shown in the right panel. miR-133b and miR-193 could significantly inhibit the MSC proliferation induced by LLLI. From 3 independent experiments. Mean ± SEM. \*P < 0.05, n = 3.



**FIG. 6.** Functional assessment of miR-193/133b. **(A, B)** Expressions of cell-cycle genes were detected by qRT-PCR in MSCs treated with miR-133b **(A)** or miR-193 **(B)** mimics or inhibitors ( $n=3$ ). **(C)** Luciferase reporter analyses of an inhibitor of growth family, member 5 (ING5) wild-type 3' untranslated region (3'UTR), as well as 1 TargetScan miR-193 site mutated (ING5 3'UTR mute) together with expression plasmids for miR-193 or a scrambled miRNA (control miRNA). miR-193 overexpression decreased luciferase activity of the wild-type but not the mutant 3'UTR where the miR-193 binding site was deleted. **(D)** ING5 mRNA expression levels were measured by qRT-PCR in the treatment MSCs. **(E)** Expression of the ING5 protein was detected by western blotting with normalization to glyceraldehyde-3 phosphate dehydrogenase (GAPDH) in transfected MSCs. The overexpression of miR-193 led to decreased ING5 expression, whereas miR-193 inhibition led to increased ING5 expression. Mean  $\pm$  SEM. \* $P < 0.05$ . \*\* $P < 0.01$ ,  $n = 3$ .



addition, the inhibition of miR-193 could increase ING5 expression (Fig. 6D, E). According to the miRNA database, the target site in the 3'-UTR of ING5 is conserved in vertebrates and partially complementary to miR-193 (Fig. 6C). The luciferase reporter system was used to test the target site. Compared with the negative control, the luciferase activity for the ING5-WT-transfected cells decreased  $\approx 60\%$  in the miR-193 mimic transfections. In addition, the decrease in luciferase activity was rescued by introducing mutations at the seed site in ING5 (Fig. 6C).

**ING5 down-regulation promotes MSCs proliferation**

To detect whether ING5 could regulate the proliferation of MSCs, we used the siRNA of ING5 to inhibit ING5 and assay the proliferation level of MSCs. qRT-PCR and western blotting showed that ING5 was significantly reduced (Fig. 7A,

B). BrdU incorporation and MTS assay showed that the inhibition of ING5 could significantly increase the proliferation of MSCs (Fig. 7C, D). Furthermore, we measured PCNA protein expression in the MSCs-Mock and MSCs-siING5 by western blot, and found that the inhibition of ING5 could increase PCNA expression in contrast to the control (Fig. 7A). In addition, we found that the inhibition of ING5 could increase CDK2 expression (Fig. 7E).

**Discussion**

Promoting MSC proliferation can facilitate the clinical translation of stem-cell therapy. Some methods have attempted to promote cell proliferation, including cytokines supplement, gene transfection, nanoparticle adhesions, and platelet-rich plasma stimulation [21–24]. LLLI treatment is a simple, economical, and effective approach that enhances cell

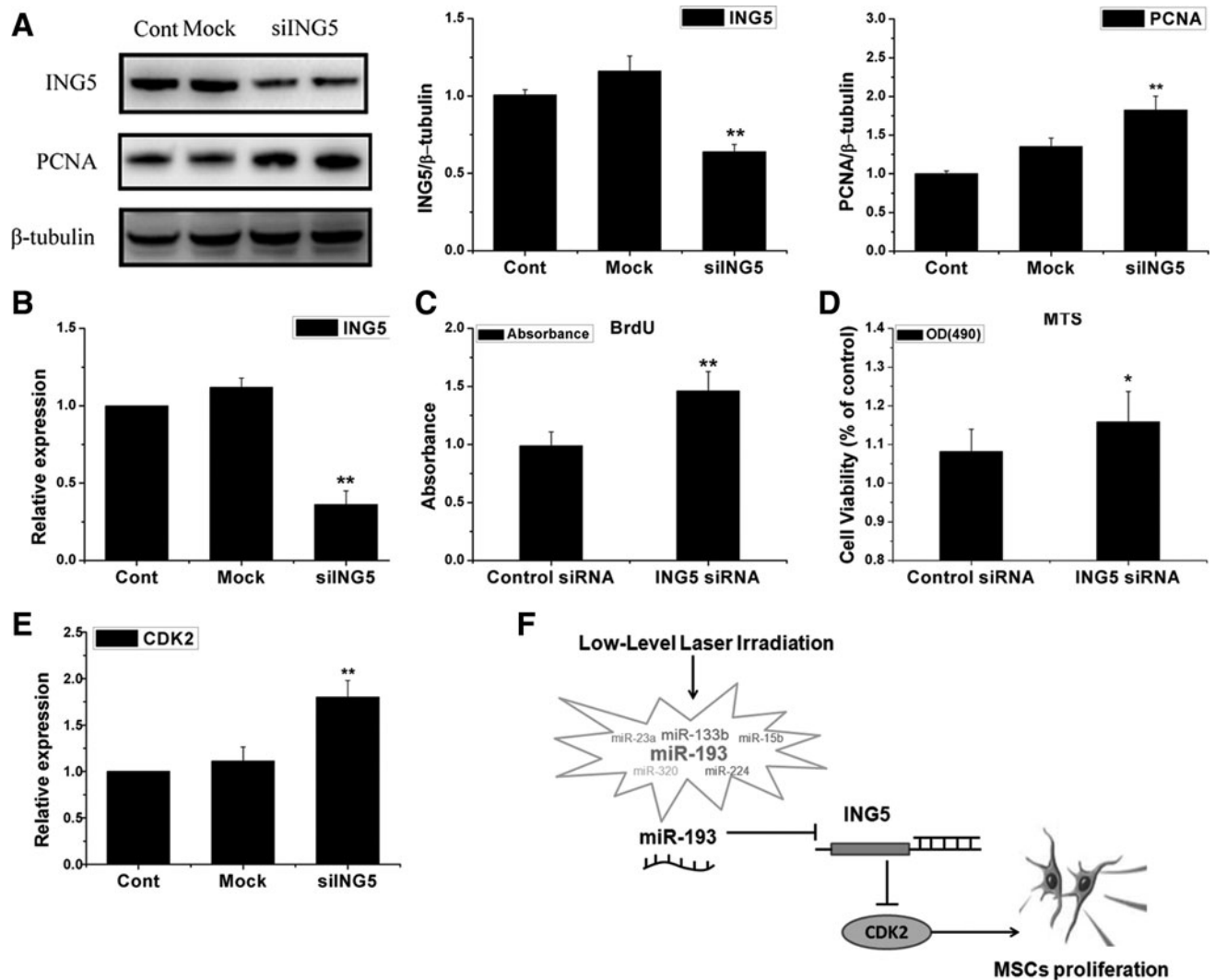


**FIG. 7.** Knockdown of ING5 by small interfering RNA promotes MSCs proliferation. (A) Expression of ING5 and proliferative cell nuclear antigen (PCNA) were determined by western blot and quantitative determination ( $n=3$ ). (B) qRT-PCR analysis for ING5 mRNA expression ( $n=3$ ). (C, D) MSCs proliferation was determined by BrdU (C) and MTS (D) ( $n=3$ ). (E) The expression of CDK2 in MSCs transfected with si-ING5 was detected by qRT-PCR. Mean  $\pm$  SEM. \* $P < 0.05$ . \*\* $P < 0.01$  compared with control siRNA groups ( $n=3$ ). (F) Proposed model of miR-193 in regulating the process of LLLI promoting MSCs proliferation.

proliferation [9]. However, the mechanisms of cell proliferation induced by LLLI are poorly understood [9]. This could be the first study that demonstrates the function of miRNA in LLLI treatment, and provides new insights in LLLI treatment. The major findings were as follows: (i) LLLI induced the activation of miR-193, and was related to cell cycle-associated gene changes; (ii) miR-193 promoted MSC proliferation, but did not affect the level of apoptosis and differentiation; and (iii) the function of miR-193 triggered by LLLI was through the ING5/CDK2 signaling pathway; the inhibited ING5 could promote MSCs proliferation. A proposed model that explains the role of miR-193 in this process is outlined in (Fig. 7F). In addition, we found that miR-193 could regulate the proliferation of hMSCs, and identified a novel approach of using miRNA therapeutics that regulate the proliferation of hMSCs, which may consequently improve efficiency in the application of hMSC for clinical practice.

It was reported that miR-193 could regulate the proliferation of the hepatocellular carcinoma target CCND1 and ETS1 [25]. In a study by Ory et al., miR-193 down-regulation suppressed tumor proliferation through p73 signaling [26]. We found that miR-193 promoted MSC proliferation by regulating the ING5-CDK2 pathway. CDK2 plays an important role in regulating the G1/S transition, and it can phosphorylate Rb and other targets in the progression through the S phase [27]. We found that the change in CDK2 after LLLI treatment for MSCs was correlated with the expression and proliferation of miR-193. In addition, we found that miR-193 could promote MSC proliferation and specifically regulate CDK2 expression. Using bioinformatic analyses, we demonstrated that ING5 was the target of miR-193 according to the following analysis. First, ING5 could directly interact with CDK2, and suppress cell proliferation [28]. Second, ING5 has been demonstrated as interacting with p53, and p53 can indirectly affect CDK2 [27,29,30]. To

clarify the association of miR-193 with ING5, we used gain-and-loss-of-function experiments. The overexpression of miR-193 reduced the ING5 protein and mRNA levels in MSCs, and the luciferase reporter assay indicated that ING5 was the direct target of miR-193. ING5 is a member of the ING family; the ING family is involved in multiple cellular functions, such as cell-cycle regulation, apoptosis, and DNA repair [31]. The overexpression of ING5 suppresses cell proliferation and delays progression of the S phase, with down-regulation of CDK2 activity [28]. ING5 has also been shown to physically interact with p53, and to decrease cell populations in the S phase [30]. Furthermore, in our experiment, the knockdown of ING5 can lead to the promotion of the proliferation of MSCs, indicating that ING5 is a possible target of miR-193 in the process of MSCs proliferation.

Furthermore, to elucidate other functions of miR-193, we detected the apoptosis and differentiation level of MSCs after them being miR-193 transfected, and we did not find a difference between the treatment and control groups.

miR-133b is expressed primarily in the skeletal muscle [32]. It has been found to enhance myoblast proliferation by repressing serum response factor (SRF) [33]. We found that miR-133b could be induced by LLLI and could promote MSC proliferation, but we did not observe changes in the SRF gene in MSCs by transfection with miR-133b (data not shown). However, miR-133b could regulate the expression of CCND1 and CDK2. These results indicated that miR-133b may regulate MSC proliferation through complicated signaling pathways; further investigations are needed to elucidate the underlying mechanism of miR-133b.

Several other miRNAs candidates also showed aberrant expression, including miR-15b, -23a, -320, and -224. miR-15b is a member of the miR-15/16 family that has been reported as regulating cell proliferation by targeting the cyclin signaling pathway in some cell lines [34]. miR-23a has been reported as promoting the proliferative potential of a gastric adenocarcinoma cell line through IL6R [35]. miR-320 may affect cell cycles through CDK6 [36] and inhibit the cell proliferation targets transferrin receptor 1 (CD71) [37]. miR-224 has been reported as enhancing the proliferation of transforming growth factor (TGF)-beta1-induced granulosa cells through targeting Smad4 [38]. However, from the gain-and-loss-of-function experiments by the MTS assay, we found that these miRNAs could not affect MSC proliferation.

In summary, LLLI was shown to promote MSC proliferation, and miRNA-193 played an important role in this proliferation effect. The present study provided new insights into the mechanisms of LLLI treatment, and also offered target miRNAs for MSC proliferation.

## Acknowledgments

This study was supported by grants from the Natural Science Foundation of China (81070099) and the Fok Ying-tong Education Foundation (121041). The authors thank Drs. Qian Zhang, Bianmei Han, and Chuangjue Cui for the excellent technical assistance rendered.

## Author Disclosure Statement

All authors have no conflict of interest.

## References

- Pittenger MF, AM Mackay, SC Beck, RK Jaiswal, R Douglas, JD Mosca, MA Moorman, DW Simonetti, S Craig and DR Marshak. (1999). Multilineage potential of adult human mesenchymal stem cells. *Science* 284:143–147.
- Baxter MA, RF Wynn, SN Jowitt, JE Wraith, LJ Fairbairn and I Bellantuono. (2004). Study of telomere length reveals rapid aging of human marrow stromal cells following *in vitro* expansion. *Stem Cells* 22:675–682.
- Xin Y, YM Wang, H Zhang, J Li, W Wang, YJ Wei and SS Hu. (2010). Aging adversely impacts biological properties of human bone marrow-derived mesenchymal stem cells: implications for tissue engineering heart valve construction. *Artif Organs* 34:215–222.
- Peplow PV, TY Chung, B Ryan and GD Baxter. (2011). Laser photobiomodulation of gene expression and release of growth factors and cytokines from cells in culture: a review of human and animal studies. *Photomed Laser Surg* 29: 285–304.
- Hou JF, H Zhang, X Yuan, J Li, YJ Wei and SS Hu. (2008). *In vitro* effects of low-level laser irradiation for bone marrow mesenchymal stem cells: proliferation, growth factors secretion and myogenic differentiation. *Lasers Surg Med* 40:726–733.
- Zhang H, JF Hou, Y Shen, W Wang, YJ Wei and S Hu. (2010). Low level laser irradiation precondition to create friendly milieu of infarcted myocardium and enhance early survival of transplanted bone marrow cells. *J Cell Mol Med* 14:1975–1987.
- Karu T. (1999). Primary and secondary mechanisms of action of visible to near-IR radiation on cells. *J Photochem Photobiol B* 49:1–17.
- Karu T, L Pyatibrat and G Kalendo. (1995). Irradiation with He-Ne laser increases ATP level in cells cultivated *in vitro*. *J Photochem Photobiol B* 27:219–223.
- Gao X and D Xing. (2009). Molecular mechanisms of cell proliferation induced by low power laser irradiation. *J Biomed Sci* 16:4.
- Huang Y, XJ Shen, Q Zou, SP Wang, SM Tang and GZ Zhang. (2011). Biological functions of microRNAs: a review. *J Physiol Biochem* 67:129–139.
- Gangaraju VK and H Lin. (2009). MicroRNAs: key regulators of stem cells. *Nat Rev Mol Cell Biol* 10:116–125.
- Tome M, P Lopez-Romero, C Albo, JC Sepulveda, B Fernandez-Gutierrez, A Dopazo, A Bernad and MA Gonzalez. (2011). miR-335 orchestrates cell proliferation, migration and differentiation in human mesenchymal stem cells. *Cell Death Differ* 18:985–995.
- Kim YJ, SH Hwang, SY Lee, KK Shin, HH Cho, YC Bae and JS Jung. (2011). miR-486-5p induces replicative senescence of human adipose tissue-derived mesenchymal stem cells and its expression is controlled by high glucose. *Stem Cells Dev* [Epub ahead of print]; DOI:10.1089/scd.2011.0429.
- Liu X, J Hou, L Shi, J Chen, J Sang, S Hu, X Cong and X Chen. (2009). Lysophosphatidic acid protects mesenchymal stem cells against ischemia-induced apoptosis *in vivo*. *Stem Cells Dev* 18:947–954.
- Li Z, H Wei, L Deng, X Cong and X Chen. (2010). Expression and secretion of interleukin-1beta, tumour necrosis factor-alpha and interleukin-10 by hypoxia- and serum-deprivation-stimulated mesenchymal stem cells. *FEBS J* 277:3688–3698.
- Wang J, R Xu, F Lin, S Zhang, G Zhang, S Hu and Z Zheng. (2009). MicroRNA: novel regulators involved in the

- remodeling and reverse remodeling of the heart. *Cardiology* 113:81–88.
17. Xie C, H Huang, X Sun, Y Guo, M Hamblin, RP Ritchie, MT Garcia-Barrio, J Zhang and YE Chen. (2011). MicroRNA-1 regulates smooth muscle cell differentiation by repressing Kruppel-like factor 4. *Stem Cells Dev* 20:205–210.
  18. Wang W, Q Jiang, H Zhang, P Jin, X Yuan, Y Wei and S Hu. (2011). Intravenous administration of bone marrow mesenchymal stromal cells is safe for the lung in a chronic myocardial infarction model. *Regen Med* 6:179–190.
  19. Hou M, KM Yang, H Zhang, WQ Zhu, FJ Duan, H Wang, YH Song, YJ Wei and SS Hu. (2007). Transplantation of mesenchymal stem cells from human bone marrow improves damaged heart function in rats. *Int J Cardiol* 115:220–228.
  20. Boiani M and HR Scholer. (2005). Regulatory networks in embryo-derived pluripotent stem cells. *Nat Rev Mol Cell Biol* 6:872–884.
  21. Vicente Lopez MA, MN Vazquez Garcia, A Entrena, S Olmedillas Lopez, M Garcia-Arranz, D Garcia-Olmo and A Zapata. (2011). Low doses of bone morphogenetic protein 4 increase the survival of human adipose-derived stem cells maintaining their stemness and multipotency. *Stem Cells Dev* 20:1011–1019.
  22. Song JS, HH Cho, BJ Lee, YC Bae and JS Jung. (2011). Role of thioredoxin 1 and thioredoxin 2 on proliferation of human adipose tissue-derived mesenchymal stem cells. *Stem Cells Dev* 20:1529–1537.
  23. Chen L, J Sun, Z Zhu, K Wu, W Li, H Liu and S Xu. (2011). The adhesion and proliferation of bone marrow-derived mesenchymal stem cells promoted by nanoparticle surface. *J Biomater Appl* [Epub ahead of print]; DOI:10.1177/0885328211414750.
  24. Duan J, W Kuang, J Tan, H Li, Y Zhang, K Hirotaka and K Tadashi. (2011). Differential effects of platelet rich plasma and washed platelets on the proliferation of mouse MSC cells. *Mol Biol Rep* 38:2485–2490.
  25. Xu C, S Liu, H Fu, S Li, Y Tie, J Zhu, R Xing, Y Jin, Z Sun and X Zheng. (2010). MicroRNA-193b regulates proliferation, migration and invasion in human hepatocellular carcinoma cells. *Eur J Cancer* 46:2828–2836.
  26. Ory B, MR Ramsey, C Wilson, DD Vadysirisack, N Forster, JW Rocco, SM Rothenberg and LW Ellisen. (2011). A microRNA-dependent program controls p53-independent survival and chemosensitivity in human and murine squamous cell carcinoma. *J Clin Invest* 121:809–820.
  27. Stein GS, AJ van Wijnen, JL Stein, JB Lian, M Montecino, SK Zaidi and C Braastad. (2006). An architectural perspective of cell-cycle control at the G1/S phase cell-cycle transition. *J Cell Physiol* 209:706–710.
  28. Zhang F, N Baumer, M Rode, P Ji, T Zhang, WE Berdel and C Muller-Tidow. (2011). The inhibitor of growth protein 5 (ING5) depends on INCA1 as a co-factor for its anti-proliferative effects. *PLoS One* 6:e21505.
  29. Gartel AL and AL Tyner. (2002). The role of the cyclin-dependent kinase inhibitor p21 in apoptosis. *Mol Cancer Ther* 1:639–649.
  30. Shiseki M, M Nagashima, RM Pedeux, M Kitahama-Shiseki, K Miura, S Okamura, H Onogi, Y Higashimoto, E Appella, J Yokota and CC Harris. (2003). p29ING4 and p28ING5 bind to p53 and p300, and enhance p53 activity. *Cancer Res* 63:2373–2378.
  31. Russell M, P Berardi, W Gong and K Riabowol. (2006). Grow-ING, Age-ING and Die-ING: ING proteins link cancer, senescence and apoptosis. *Exp Cell Res* 312:951–961.
  32. Small EM, RJ Frost and EN Olson. (2010). MicroRNAs add a new dimension to cardiovascular disease. *Circulation* 121:1022–1032.
  33. Chen JF, EM Mandel, JM Thomson, Q Wu, TE Callis, SM Hammond, FL Conlon and DZ Wang. (2006). The role of microRNA-1 and microRNA-133 in skeletal muscle proliferation and differentiation. *Nat Genet* 38:228–233.
  34. Xia H, Y Qi, SS Ng, X Chen, S Chen, M Fang, D Li, Y Zhao, R Ge, G Li, Y Chen, ML He, HF Kung, L Lai and MC Lin. (2009). MicroRNA-15b regulates cell cycle progression by targeting cyclins in glioma cells. *Biochem Biophys Res Commun* 380:205–210.
  35. Zhu LH, T Liu, H Tang, RQ Tian, C Su, M Liu and X Li. (2010). MicroRNA-23a promotes the growth of gastric adenocarcinoma cell line MGC803 and downregulates interleukin-6 receptor. *FEBS J* 277:3726–3734.
  36. Duan H, Y Jiang, H Zhang and Y Wu. (2010). MiR-320 and miR-494 affect cell cycles of primary murine bronchial epithelial cells exposed to benzo[a]pyrene. *Toxicol In Vitro* 24:928–935.
  37. Schaar DG, DJ Medina, DF Moore, RK Strair and Y Ting. (2009). miR-320 targets transferrin receptor 1 (CD71) and inhibits cell proliferation. *Exp Hematol* 37:245–255.
  38. Yao G, M Yin, J Lian, H Tian, L Liu, X Li and F Sun. (2010). MicroRNA-224 is involved in transforming growth factor-beta-mediated mouse granulosa cell proliferation and granulosa cell function by targeting Smad4. *Mol Endocrinol* 24:540–551.

Address correspondence to:

*Dr. Hao Zhang*

*State Key Laboratory of Cardiovascular Medicine*

*Department of Surgery*

*Fuwai Hospital & Cardiovascular Institute*

*Chinese Academy of Medical Sciences*

*Peking Union Medical College*

*Research Center for Cardiac Regenerative Medicine*

*Ministry of Health*

*167 Beilishi Road*

*Beijing 100037*

*China*

*E-mail: drzhanghao@yahoo.com*

Received for publication December 13, 2011

Accepted after revision March 2, 2012

Prepublished on Liebert Instant Online March 2, 2012